On the relationship between azimuthal anisotropy from shear wave splitting and surface wave tomography

T. W. Becker,[1] S. Lebedev,[2] and M. D. Long[3]

Received 24 July 2011; revised 26 September 2011; accepted 8 November 2011; published 14 January 2012.

[1] Seismic anisotropy provides essential constraints on mantle dynamics and continental evolution. One particular question concerns the depth distribution and coherence of azimuthal anisotropy, which is key for understanding force transmission between the lithosphere and asthenosphere. Here, we reevaluate the degree of coherence between the predicted shear wave splitting derived from tomographic models of azimuthal anisotropy and that from actual observations of splitting. Significant differences between the two types of models have been reported, and such discrepancies may be due to differences in averaging properties or due to approximations used in previous comparisons. We find that elaborate, full waveform methods to estimate splitting from tomography yield generally similar results to the more common, simplified approaches. This validates previous comparisons and structural inversions. However, full waveform methods may be required for regional studies, and they allow exploiting the back-azimuthal variations in splitting that are expected for depth-variable anisotropy. Applying our analysis to a global set of *SKS* splitting measurements and two recent surface wave models of upper-mantle azimuthal anisotropy, we show that the measures of anisotropy inferred from the two types of data are in substantial agreement. Provided that the splitting data is spatially averaged (so as to bring it to the scale of long-wavelength tomographic models and reduce spatial aliasing), observed and tomography-predicted delay times are significantly correlated, and global angular misfits between predicted and actual splits are relatively low. Regional anisotropy complexity notwithstanding, our findings imply that splitting and tomography yield a consistent signal that can be used for geodynamic interpretation.

Citation: Becker, T. W., S. Lebedev, and M. D. Long (2012), On the relationship between azimuthal anisotropy from shear wave splitting and surface wave tomography, *J. Geophys. Res.*, *117*, B01306, doi:10.1029/2011JB008705.

1. Introduction

[2] Earth's structure and tectonic evolution are intrinsically linked by seismic anisotropy in the upper mantle and lithosphere, where convective motions are recorded during the formation of lattice-preferred orientation (LPO) fabrics under dislocation creep [e.g., *Nicolas and Christensen*, 1987; *Silver*, 1996; *Long and Becker*, 2010]. However, within the continental lithosphere, seismically mapped anisotropy appears complex [e.g., *Fouch and Rondenay*, 2006]. Transitions between geologically recent deformation and frozen-in anisotropy from older tectonic motions are reflected in layering [e.g., *Plomerova et al.*, 2002; *Yuan and Romanowicz*, 2010] and the stochastic character of azimuthal anisotropy in geological domains of different age [*Becker et al.*, 2007a, 2007b; *Wüstefeld et al.*, 2009]. Regional studies indicate intriguing variations of azimuthal anisotropy with depth, which may reflect decoupling of deformation or successive deformation episodes recorded at different depths [e.g., *Savage and Silver*, 1993; *Pedersen et al.*, 2006; *Marone and Romanowicz*, 2007; *Deschamps et al.*, 2008a; *Lin et al.*, 2011; *Endrun et al.*, 2011]. All of these observations hold the promise of yielding a better understanding of the long-term behavior of a rheologically complex lithosphere, including changes in plate motions and the formation of the continents.

[3] Ideally, one would like to have a complete, three-dimensional (3-D) model of the full (21 independent components) elasticity tensor for such structural seismology studies. Fully anisotropic inversions are feasible, in principle [cf. *Montagner and Nataf*, 1988; *Panning and Nolet*, 2008; *Chevrot and Monteiller*, 2009], particularly if mineral physics and petrological information are used to reduce the dimensionality of the model parameter space [*Montagner and Anderson*, 1989; *Becker et al.*, 2006a]. However, often the sparsity of data requires, or simplicity and convenience demand, restricting the analysis to joint models that constrain only aspects of seismic anisotropy, for example the azimuthal kind, on which we focus here.

[1]Department of Earth Sciences, University of Southern California, Los Angeles, California, USA.
[2]Dublin Institute for Advanced Study, Dublin, Ireland.
[3]Department of Geology and Geophysics, Yale University, New Haven, Connecticut, USA.

0148-0227/12/2011JB008705

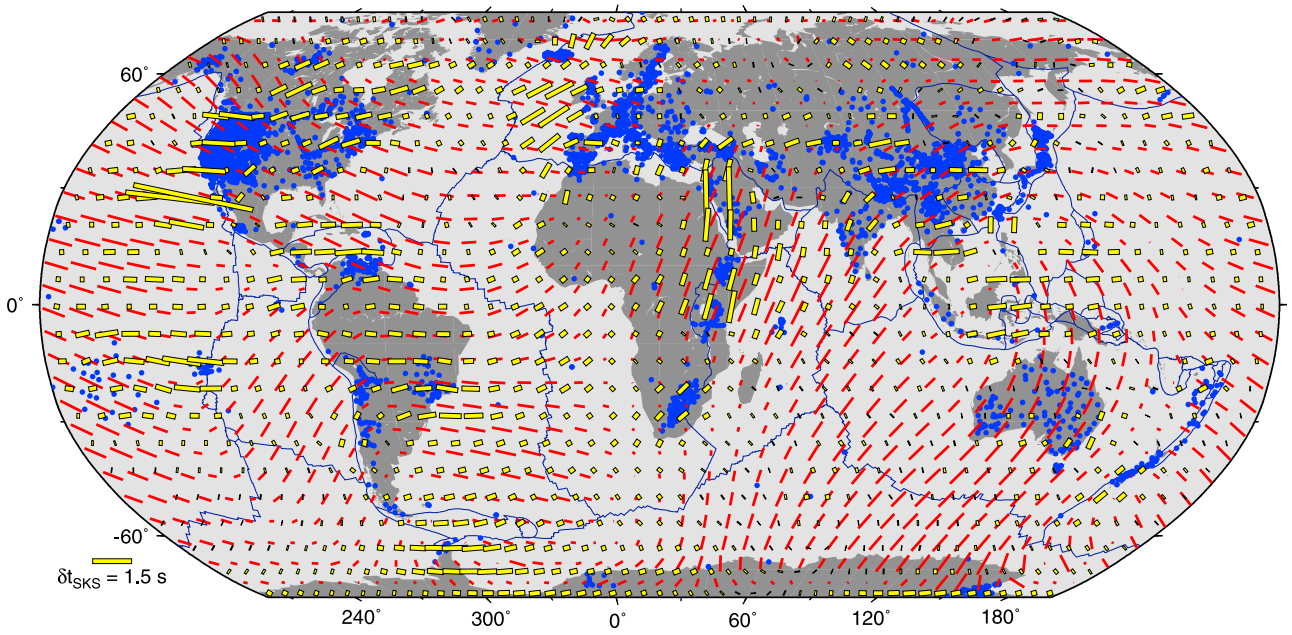

Figure 1. Distribution of *SKS* splitting in our merged database (blue dots, with 5159 station-averaged entries) and damped, $L = 20$, generalized spherical harmonics representation of *SKS* splitting (yellow sticks, see Appendix A), shown on top of the 200 km depth 2Ψ azimuthal anisotropy from *Lebedev and van der Hilst* [2008] (red sticks, equation (3)). Splitting measurements are mainly based on compilations by *Silver* [1996], *Fouch* [2003], and *Wüstefeld et al.* [2009], with additional references and data available at http://geodynamics.usc.edu/~becker/. Plate boundaries here and subsequently are from *Bird* [2003].

[4] For azimuthal anisotropy, hexagonal crystal symmetry is assumed with symmetry axis in the horizontal plane yielding a fast, v_{SV1}, and a slow, v_{SV2}, propagation direction for vertically polarized shear waves. Surface (Rayleigh) wave observations can constrain the anisotropic velocity anomaly, $G/L = (v_{SV1} - v_{SV2})/v_{SV}$, and the fast, Ψ, orientation for shear wave propagation. Here, G and L are the relevant elastic constants and v_{SV} the mean velocity, as defined by *Montagner et al.* [2000]. Given the dispersive nature of surface waves, phase velocity observations from different periods can be used to construct 3-D tomographic models for G/L and Ψ. Particularly in regions of poor coverage, tomographic models can be affected by the tradeoff between isotropic and anisotropic heterogeneity [e.g., *Tanimoto and Anderson*, 1985; *Laske and Masters*, 1998], which typically limits the lateral resolution to many hundreds of kilometers in global models [e.g., *Nataf et al.*, 1984; *Montagner and Tanimoto*, 1991; *Debayle et al.*, 2005; *Lebedev and van der Hilst*, 2008].

[5] This approach can then be contrasted with observations of shear wave splitting [e.g., *Ando et al.*, 1983; *Vinnik et al.*, 1984; *Silver and Chan*, 1988], typically from teleseismic *SKS* arrivals. A split shear wave is direct evidence for the existence of anisotropy. In its simplest form, a splitting measurement provides information on the azimuthal alignment of the symmetry axis, ϕ, of a single, hexagonally anisotropic layer and the delay time that the wave has accumulated between the arrival of the fast and the slow split S wave pulse, δt. With Fresnel-zone widths of ~100 km, splitting measurements have relatively good lateral, but poor depth resolution, suggesting that body and surface wave based anisotropy models provide complementary information (Figure 1).

[6] An initial global comparison between different azimuthal anisotropy representations was presented by *Montagner et al.* [2000] who compared the *SKS* splitting compilation of *Silver* [1996] with the predicted anisotropy, ϕ' and $\delta t'$, based on tomography by *Montagner and Tanimoto* [1991]. *Montagner et al.* [2000] found a poor global match with a bimodal coherence, $C(\alpha)$, as defined by *Griot et al.* [1998], which suggested typical angular deviations, α, between ϕ from *SKS* and ϕ' based on integration of Ψ and G/L from tomography of $\alpha \sim \pm 40°$, where $\alpha = \phi' - \phi$. An updated study was conducted by *Wüstefeld et al.* [2009], who used their own greatly expanded compilation of *SKS* splitting results and compared the coherence of azimuthal anisotropy with the predicted ϕ' obtained from the model of *Debayle et al.* [2005] on global and regional scales. *Wüstefeld et al.* [2009] conclude that the global correlation between the two representations of anisotropy was in fact "substantial." This improved match, with a more pleasing, single peak of C at zero lag, $\alpha = 0$, was attributed to improved surface wave model resolution and better global coverage by *SKS* studies. *Wüstefeld et al.* [2009] also explore a range of ways to represent ϕ from *SKS*. Their best global coherence values were, however, $C(0) \approx 0.2$, which is only ~1.7 times the randomly expected coherence at equivalent spatial representation. While no correlation values were provided, a scatterplot of actual δt and $\delta t'$ from integration of G/L [*Wüstefeld et al.*, 2009, Figure 9] also shows little correlation of anisotropy strength.

[7] One concern with any studies that perform a joint interpretation of splitting and anisotropy tomography is that the shear wave splitting measurement does not represent

a simple average of the azimuthal anisotropy along the raypath [e.g., *Rümpker et al.*, 1999; *Saltzer et al.*, 2000; *Silver and Long*, 2011]. Typically, the method proposed by *Montagner et al.* [2000] for the case of small anisotropy and long period waves is used to compute predicted splitting from tomographic models [e.g., *Wüstefeld et al.*, 2009], and this basically represents a vectorial averaging, weighing all layers evenly along the ray path. In continental regions, fast orientations of azimuthal anisotropy and amplitudes may vary greatly with depth over the top ~400 km of the upper mantle. We therefore expect significant deviations from simple averaging [*Saltzer et al.*, 2000] and, moreover, a dependence of both predicted delay time and fast azimuths of the splitting measurement on back-azimuth of the shear wave arrival [e.g., *Silver and Savage*, 1994; *Rümpker and Silver*, 1998; *Schulte-Pelkum and Blackman*, 2003]. It is therefore important to test the assumptions inherent in the *Montagner et al.* [2000] averaging approach, both to understand the global coherence between body and surface wave-based models of seismic anisotropy and to verify that regional, perhaps depth-dependent, deviations between the two are not partially an artifact of methodological simplifications.

[8] Here, we analyze two recent tomographic models of global azimuthal anisotropy and show what kinds of variations in splitting measurements can be expected based on a more complete treatment of predicted shear wave splitting that incorporates appropriate depth-integration. We show that, overall, the simplified predictions are suitable, but local variations between methods can be significant. We also reassess the match between predicted and actual splitting and show that smoother representations of Earth structure appear to match long-wavelength-averaged splitting quite well, albeit at much reduced amplitudes.

2. Splitting Estimation Methods

[9] Our goal is to estimate the predicted shear wave splitting from a tomographic model of seismic anisotropy in the Earth. In theory, this requires a 3-D representation of the full elasticity tensor along the raypath of whichever shear wave is considered, for *SKS* from the core mantle boundary to the surface. In practice, we focus on the uppermost mantle where most mantle anisotropy is concentrated [e.g., *Panning and Romanowicz*, 2006; *Kustowski et al.*, 2008], as expected given the formation of LPO under dislocation creep [*Karato*, 1992; *Becker et al.*, 2008; *Behn et al.*, 2009]. We will also not consider lateral variations of anisotropy on scales smaller than the Fresnel zone. This would require fully three-dimensional wave propagation methods [e.g., *Chevrot et al.*, 2004; *Levin et al.*, 2007] but is not warranted given the resolution afforded by tomographic models.

[10] The computation of shear wave splitting parameters from actual seismograms involves estimating the fast "axes" (i.e., the apparent fast polarization direction) and the delay time, and there are at least three ways of computing the equivalent, predicted ϕ' and $\delta t'$ parameters from tomography: *Montagner et al.* [2000] averaging of G/L azimuthal anomalies, computing splitting using the Christoffel matrix approach for an average tensor, and full waveform synthetic splitting.

2.1. Montagner Averaging of G/L Azimuthal Anomalies

[11] In the case of small anisotropy and long period waves (period $T > 10$ s), the predicted splitting for a tomographic model can be computed as [*Montagner et al.*, 2000]

$$\delta t' = \sqrt{f_c^2 + f_s^2} \quad \text{and} \quad \phi' = \frac{1}{2}\tan^{-1}\left(\frac{f_s}{f_c}\right), \tag{1}$$

where the vector components $f_{c,s}$ are the depth integrals (assuming a vertical path)

$$f_{c,s} = \int_0^a \sqrt{\frac{\rho}{L}}\frac{G_{c,s}}{L}dz = \int_0^a \frac{1}{v_{SV}}\frac{G_{c,s}}{L}dz, \tag{2}$$

a is the length of the path, $v_{SV} = \sqrt{L/\rho}$, ρ density, and c and s indices indicate the azimuthal cos and sin contributions to anisotropy, as follows: The relevant components of the elasticity tensor that determine the splitting are G/L with $G = \sqrt{G_c^2 + G_s^2}$, and the ratios $G_{c,s}/L$ relate to the typical parameterization of azimuthal-anisotropy tomography models

$$\frac{dv_{SV}}{v_{SV}} \approx A_0 + A_c \cos 2\Psi + A_s \sin 2\Psi \tag{3}$$

as

$$\frac{G_{c,s}}{L} = 2A_{c,s}. \tag{4}$$

Here, dv_{SV} is total the velocity anomaly with respect to a one-dimensional reference model, A_0 the isotropic velocity anomaly, and all higher order, 4Ψ, terms are neglected. Assuming vertical incidence and neglecting any effects due to isotropic anomalies A_0, the predicted splitting at every location can then be approximated by integration of the $A_{c,s}$ terms over depth, z, as in equation (2). To check if the assumptions of small anisotropy and long-period filtering might be violated on Earth and in actual *SKS* measurements and to estimate the degree of variability of ϕ' and $\delta t'$ with back-azimuth, we also compute splitting using two more elaborate methods.

2.2. Christoffel Matrix From Averaged Tensors

[12] We assume that the "real" anisotropic Earth can be approximated using the information in the azimuthally anisotropic surface wave models and convert the $A_{c,s}$ factors from tomography underneath each location into complete anisotropic tensors, $\mathsf{C}(z)$, as a function of depth. To obtain $\mathsf{C}(z)$, we tested several approaches, most simply aligning a best-fit, hexagonal approximation to an olivine-enstatite tensor in the horizontal plane, and then scaling the anisotropy such that the effective, transversely isotropic ("splitting") anomaly in the horizontal plane, δ^h_{TI}, corresponds to $2A_{c,s} = G/L$ from tomography at that depth (using the decomposition of *Browaeys and Chevrot* [2004]). We also consider an identically aligned, but fully anisotropic, depth-dependent olivine-enstatite tensor (as used in the work of *Becker et al.* [2006a]), again scaled such that $\delta^h_{TI} = 2A_{c,s}$, which adds orthorhombic symmetry components. Last, to explore the effect of dipping symmetry axes, we scaled down the full, hexagonally approximated olivine-enstatite tensor anisotropy by a factor of four to δ^o_{TI} and then aligned

the tensor at a dip angle of β out of the horizontal plane such that $\cos(\beta)\delta^o_{TI} = \delta^h_{TI} = 2A_{c,s}$ matched the azimuthal anisotropy from tomography, rescaling in an iterative step, if needed. The latter two approaches (nonhexagonal or dipping symmetry) are expected to yield a more complex splitting signal with back-azimuthal variations [e.g., *Schulte-Pelkum and Blackman*, 2003; *Browaeys and Chevrot*, 2004].

[13] From this anisotropic model where, for each location under consideration, we have estimates of $\mathsf{C}(z)$ at each layer, we first compute a depth-averaged tensor $\tilde{\mathsf{C}}$, using arithmetic, i.e., Voigt, averaging. From this average tensor, we then compute splitting as a function of incidence and back-azimuth based on the Christoffel equation [e.g., *Babuska and Cara*, 1991] using the implementation of *Schulte-Pelkum and Blackman* [2003]. Differently from the *Montagner et al.* [2000] averaging, this method not only yields ϕ' and $\delta t'$ but also simplified estimates of the variations of both parameters as a function of back-azimuth, σ_ϕ and $\sigma_{\delta t}$. When computing back-azimuthal variations, we fix the incidence angle to 5°, as a typical value for *SKS*. When averaging $\mathsf{C}(z)$ for the Christoffel approach, we use constant weights for each layer, even though we expect surface-near regions to contribute more strongly in reality [e.g., *Rümpker et al.*, 1999; *Saltzer et al.*, 2000], because such wave propagation effects can be captured more fully by the method that is discussed next.

2.3. Full Waveform Synthetic Splitting

[14] Last, we also follow the approach suggested by *Hall et al.* [2000] to obtain splitting from geodynamic predictions of anisotropy, accounting for the full waveform complexities given the depth-dependent $\mathsf{C}(z)$ model we can construct at each location using the method described above. Following *Becker et al.* [2006b], we first use a layer matrix computation that accounts for the depth dependence of anisotropy by assigning a constant tensor for each layer that the ray path crosses. This method assumes that lateral variations in material properties are small on the wavelengths of a Fresnel zone. Our waveform modeling approach is based on *Kennett* [1983], with extensions by *Booth and Crampin* [1985] and *Chapman and Shearer* [1989], and yields a pulse train. This is then bandpass-filtered to construct synthetic seismograms in *SKS*-typical bands of $T \approx 7$ s center period. We use mainly the cross-correlation method [e.g., *Fukao*, 1984; *Bowman and Ando*, 1987], implemented following *Levin et al.* [1999], to automatically measure splitting from modeled waveforms, scanning through the full back-azimuth of the incoming *SKS* waves. We discard nulls and poor measurements and report both the mean ("best") and standard deviations (σ_ϕ and $\sigma_{\delta t}$) of the inferred $\delta t'$ and ϕ' (for details, see *Becker et al.* [2006b]).

[15] The cross-correlation method is equivalent to the transverse-component minimization method [*Silver and Chan*, 1988] for a single horizontal layer in the absence of noise. However, cross-correlation should perform better in the case of multiple layers of anisotropy [*Levin et al.*, 1999; *Long and van der Hilst*, 2005] as is the case for some locales where Ψ rotates quite widely with depth (Figure 2). While detailed results of the splitting measurement depend on analysis choices such as filtering, windowing, and measurement method, general results are usually consistent [e.g., *Long and van der Hilst*, 2005; *Wüstefeld and Bokelmann*, 2007]. However, to test this assumption in the framework of our automated splitting setup, we also present some cases where splits were computed using the cross-convolution routine ah_cross_conv_1 of *Menke and Levin* [2003], which has a slightly different optimization strategy from our implementation of *Levin et al.* [1999] (all software and data used here are provided at http://geodynamics.usc.edu/~becker/). More importantly, we also experiment with the waveform filtering, allowing for longer periods of $T \approx 12.5$ s and $T \approx 15$ s to test how the approximation of *Montagner et al.* [2000] is affected.

3. Azimuthal Anisotropy Observations and Models

3.1. Shear Wave Splitting Database

[16] We maintain our own compilation of shear wave splitting measurements, mainly based on the efforts by *Silver* [1996] and *Fouch* [2003] but subsequently updated by addition of regional studies and now holding 9635 entries. For this study, our database was merged with that of *Wüstefeld et al.* [2009] which had 4778 entries as of May 2011, yielding a total of 14,326 splits. Our compilation includes measurements carried out by many different authors, and individual studies differ in the measurement methods used, processing choices such as event selection, filtering, windowing, and back-azimuthal coverage. Given such methodological concerns and the possibly large back-azimuth variation of splitting parameters if anisotropy is complex underneath a single station, it would be desirable to have a consistent measurement and waveform filtering strategy, and to take into account back-azimuth information. However, we only have event and method information for a small subset of the splits, which is why we discard this information subsequently. If we station-average the splits (using an arithmetic, vectorial mean of all nonnull splits, taking the 180° periodicity of ϕ into account), we are left with 5159 mean splitting values on which we base our analysis (Figure 1). Such averaging is expected to also reduce the effect of some of the inconsistencies of the splitting database, for example the mix between already station-averaged and individual splits reported. (An electronic version of this *SKS* compilation can be found at http://geodynamics.usc.edu/~becker/.)

[17] We will consider both this complete station-averaged data set and spatially averaged versions of it. Several averaging and interpolation approaches for shear wave splitting data have been discussed [e.g., *Wüstefeld et al.*, 2009]. Here, we use one global basis-function approach and a simple averaging scheme that does not make any assumptions about the statistical properties of the data. For a global, smoothed representation we use generalized spherical harmonics as implemented by *Boschi and Woodhouse* [2006]. For consistency with the tomographic models (see below), we use a maximum degree $L = 20$ (individual degree $\ell \in [2;L]$ for a 2Ψ type of signal) and perform a least-squares fit to the station-averaged splits (Appendix A). Such global representations assume that the field represented by the splits is smooth (which it is not, but it may be seen as such by the tomographic models) and will extrapolate into regions without data.